Polarization Switching Dependence of VCSEL on Variable Polarization Optical Feedback

Salam Nazhan, *Member, IEEE*, and Zabih Ghassemlooy, *Senior Member, IEEE*

***Abstract*— In this paper, the influence of variable-angle polarization-rotated optical feedback on the polarization switching properties of vertical-cavity surface-emitting lasers (VCSELs) is investigated theoretically and experimentally. The optical feedback (OF) level and the rotated polarization angle θ_p of OF are considered. Two configurations of OF are used to re-injected parallel and orthogonal polarization modes back into the VCSEL. For the parallel OF, it is shown that polarization switching (PS) of VCSELs' modes can occur at a fixed feedback level and bias current with variable θ_p. However, in case of orthogonal optical feedback, PS occurs only at certain values of θ_p, particularly when the intensities of two polarization modes become comparable with each other. In the theoretical model for both OF conditions, there is good agreement between the experimental measurements and recent theoretical results reported in the literature.**

***Index Terms*— Vertical-cavity surface emitting lasers (VCSELs), variable polarization angle, optical feedback, polarization switching (PS).**

I. Introduction

VERTICAL-CAVITY surface-emitting lasers (VCSELs) are attractive light sources because of their desirable characteristics, such as a low threshold current, single-longitudinal operation and circular output-beam profile, which make VCSELs promising devices in many applications [1]–[4]. However, VCSELs are very sensitive to the optical feedback (OF) because of their short cavity length and a large emitting area. Several theoretical and experimental studies have been made to study the polarization properties of VCSELs under different OF conditions [5]–[9]. OF strongly affects the dynamics of VCSEL devices, and has been the subject of extensive research activities in recent years. However, the majority of previous studies have focused on the influence of conventional OF on the dynamical characteristics and stability of the VCSELs [5], [10]–[12]. The VCSELs spectral characteristics and their controllable polarization switching (PS) characteristics have also been investigated [13]–[16]. Polarization properties of semiconductor lasers [17], [18] subject to the conventional OF [19] and with the variable angle of polarization based OF have been studied both experimentally and theoretically [1], [20]–[23].

In [21] the variable polarization rotation angle of OF was implemented to experimentally investigate the dynamics of conventional edge-emitting lasers (EELs). In [22], the Lang-Kobayashi equations were extended to show the influence of variable-angle polarization-rotated OF on the polarization properties of 1550 nm VCSELs. Under a relatively low feedback ratio, OF plays a less important role than the gain effect. Moreover, it was predicted that larger rotated polarization angle θ_p leads to PS and mostly emitting the suppressed mode. On the other hand, with regards to higher feedback ratio, the feedback strength competes with the gain for the dominant effect [22]. In our recent study, PS properties of VCSEL when subjected to the modulation signal with a variable angle and OF was reported in [24]. The results showed that the modulation parameters (i.e., frequency f_mod and the modulation-depth M_mod) can results in elimination of PS in VCSELs. Recently we have experimentally investigated the harmonics distortion dependency of the chaotic signal dynamics of VCSEL on orthogonal polarization [25] and on the rotated angle, respectively [3] of the OF. However, an experimental study supported by predicted polarization properties of VCSELs subject to θ_p has not yet been reported.

Moreover, Xiang [22] extend the Lang-Kobayashi equations to consider the OF effects when using a 1550 nm VCSEL. In this paper, the spin-flip model is extended to study the rotated OF effects for VCSEL at a wavelength of 850 nm, which shows in general a good agreement between predicted and measured results. Therefore, two different models, Lang-Kobayashi and spin-flip model, have good production agreement on VCSELs having different wavelengths, which can be of interest for the researchers working with VCSEL or using it. Furthermore, this work provides, for the first time, both theoretically and experimentally investigation of the effects of variable θ_p OF on PS of an 850 nm VCSEL using two configurations (A) and (B) for re-injecting the light back into the VCSEL. In the configuration A, parallel polarization OF (i.e., XP), with respect to the fundamental polarization VCSEL's mode, is re-injected back into the device. While in the configuration B, parallel and orthogonal polarization OF (i.e., XP and YP) are re-launched into the VCSEL. The results show that, at higher OF levels smaller θ_p is required to achieve PS in the VCSEL. Polarization stability of VCSELs modes is an important factor for mid and long range optical communications that use VCSELs as transmitter, where error

Manuscript received March 28, 2017; revised June 13, 2017; accepted June 16, 2017. Date of publication June 22, 2017; date of current version July 7, 2017. This work was supported by the Scholarship offered by the College of Engineering/University of Diyala/Iraq. *(Corresponding author: Salam Nazhan.)*

S. Nazhan is with the Power and Electrical Machines Department, College of Engineering, University of Diyala, Baqubah, Iraq (e-mail: salam_nzhan@yahoo.com).

Z. Ghassemlooy is with the Optical Communications Research Group, NCRLab. Faculty of Engineering and Environment, Northumbria University, NE1 8ST Newcastle upon Tyne, U.K.

Color versions of one or more of the figures in this paper are available online at http://ieeexplore.ieee.org.

Digital Object Identifier 10.1109/JQE.2017.2718550

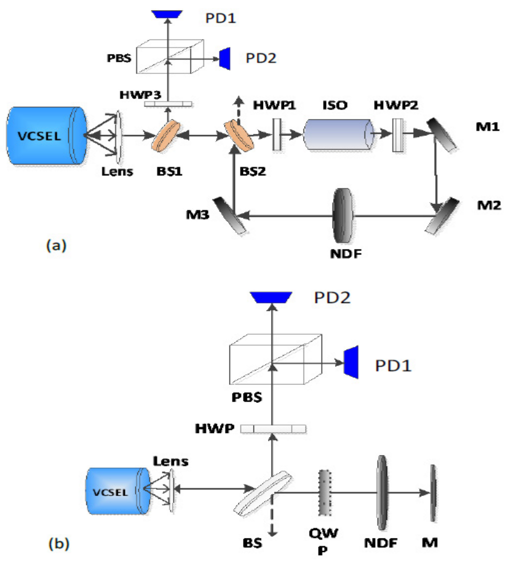

Fig. 1. Experimental setups: (a) configuration A, and (b) configuration B; BS: beam splitter. HWP: half wave plate. ISO: optical isolator. M: mirror. NDF: neutral density filter. PBS: polarized beam splitter. PD: photo-detector. PM: power meter. QWP: quarter wave plate.

free data transmission can be achieved with higher polarization stability [26].

The remainder of this paper is organized as follows; In section II the experimental setups details are given. In section III, results and discussion are presented, which contains the polarization resolved light-current (L-I) characteristics of free-running VCSEL, as well as the effect of OF level and variable polarization angle. In section IV, the numerical results of configurations A and B are given. Finally, in section V, brief conclusions are made.

II. Experimental Arrangement

Here two different OF configurations were considered: A and B, which are illustrated in Figs. 1(a) and (b), respectively. A premium 850 nm single mode VCSEL (Avalon photonics UK Components Ltd) with a threshold current of 3.9 mA and a side-mode suppression ratio (SMSR) >33dB was used. The VCSEL was driven by a DC source (7651 YOKOGAWA) and was temperature controlled using a thermoelectric temperature controller (TED 200) to within 0.01 °C. With regards to the configuration A, a half wave plate (HWP 1) was used to select the polarization direction of VCSEL's mode (XP), and an isolator (ISO) with an attenuation >40 dB was utilised to ensure that the beam from the VCSEL passed though the OF loop in one direction, and then was re-injected back into the VCSEL. The HWP2 was used to rotate the polarization direction from 0° (maximum power passed through HWP2) to 90° at a rotating increment angle of 5°. The OF level was adjusted using a neutral density filter (NDF). The power meter (PM) was used to measure the OF level. The laser output power was measured using two photo-detectors (PD1, PD2) via HWP3 and a polarization beam splitter (PBS). The detectors (Newport model AD-70xr) used have a 6 GHz bandwidth.

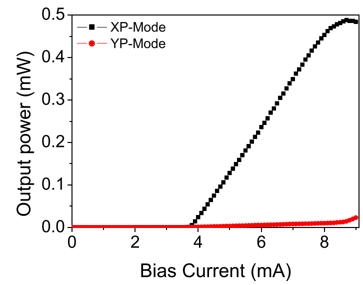

Fig. 2. Polarization-resolved L-I curve of free-running VCSEL.

Non-polarizing beam splitters BS1 & 2 were used to direct the VCSEL's output to the photodetectors (PD1 and PD2) and to the OF loop, respectively. In contrast, in the configuration B, where the two polarization modes are re-injected back into the VCSEL, a quarter wave plate (QWP) was used to rotate the OF of the XP and YP modes.

III. Results and Discussion

A. The Effect of Optical Feedback Level

Fig. 2 displays the polarization resolved L-I characteristics of the free-running VCSEL. The VCSEL starts to lase at a threshold current of ~3.9 mA with XP (black curve) and YP (red curve) modes being the dominant and suppressed modes, respectively. No PS was observed in the entire range of the bias current I_B. Note that, I_B was fixed at 6 mA (i.e., mid-point of the L-I curve) for all the experiments with results depicted in Figs. (3-7). In this way, it was ensured that the YP mode was significantly suppressed relative to the XP mode.

In this work the OF level was defined as the ratio of the feedback power (measured at BS2 and BS for configurations A and B, respectively) to the total VCSEL output power.

1) Case A: First, consideration was given to study the polarization properties of VCSEL at $\theta_p = 0°$ (i.e., parallel OF (XP) to the solitary VCSEL mode). Figure 3(a) shows that for $\theta_p = 0°$ VCSEL emits a single XP mode over the entire range of OF level. This is because at $\theta_p = 0°$ the XP mode will attain all the OF light.

In Fig. 3(b) for $\theta_p = 45°$, the intensities of both modes increase with the XP mode remaining the dominant mode. In this case, the OF was shared equally between the XP and YP modes. For $\theta_p > 45°$, the intensities of the XP and XY modes decrease and increase, respectively. In this case the XP (YP) mode loses (gains) the OF light over the range of the OF. In addition, for $\theta_p > 45°$ it can be noted from Figs. 3(c, d) that both XP and YP intensities are close to each other, which leads to PS occurring at higher OF levels (i.e., -14 dB). In this case, in contrast to the XP mode, the YP mode experiences more OF light with increased θ_p.

2) Case B: The intensities of the XP and YP modes versus the OF level for the configuration B are shown in Fig. 4. For $\theta_p = 0°$ as in Fig 4(a), VCSEL exhibits a single polarization mode (XP), as in Fig. 3(a). The XP mode is the dominant mode even when it is subjected to a strong OF level. Note that, I_B was fixed at a value to ensure that the YP mode was highly

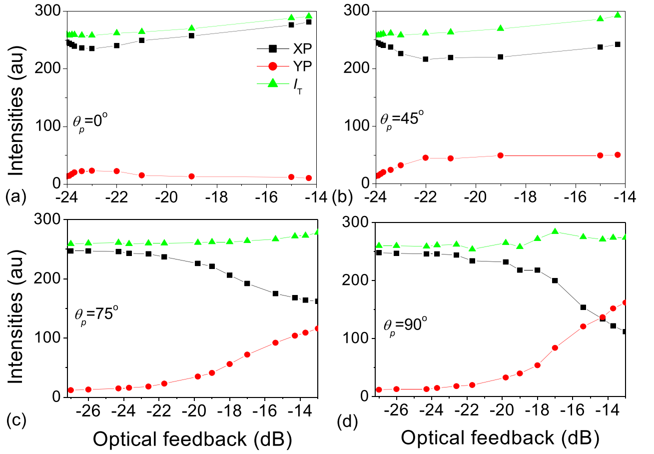

Fig. 3. Polarization-resolved intensities versus optical feedback for the configuration A (XP-OF) for θ_p of (a) 0°, (b) 45°, (c) 75° and (d) 90°.

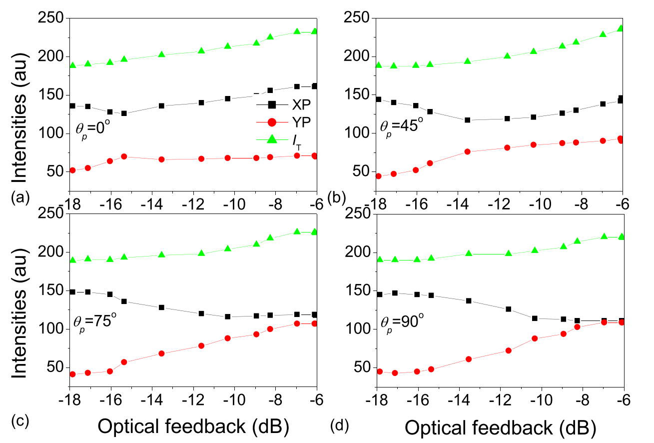

Fig. 4. Polarization-resolved intensities versus optical feedback for the configuration B for θ_p of: (a) 0°, (b) 45°, (c) 75°, and (d) 90°.

suppressed, so no light was reflected to the YP mode (i.e., zero feedback). In Fig. 4(b) both intensities of XP and YP mode exhibit similar behaviour, gradually increasing with the OF level. At θ_p of 45°, both modes are subjected to an equal OF level. Furthermore, as θ_p increases the XP (YP) mode loses (obtains) more OF light. At the comparable feedback strength level both XP and YP have almost the same intensities behaviours.

Fig. 4(c, d), illustrate further enhancement of the YP mode as well as the total intensity, whilst the XP mode intensity decreases slightly, with increasing OF level over the entire range for $\theta_p = 75°$ and 90°. For the configuration B and over the entire range of OF, the XP mode is always the dominant mode for all values of θ_p, and with no PS, as was theoretically predicted in [22]. This is mainly attributed to the gain of the YP mode being less than the gain of the XP mode, (see Fig. 7)

B. The Effects of Variable Polarization Angle

Next, the effects of varying θ_p of OF on the PS of VCSEL are considered. In this case, both the OF level and I_B were fixed and θ_p was varied from 0° to 90°.

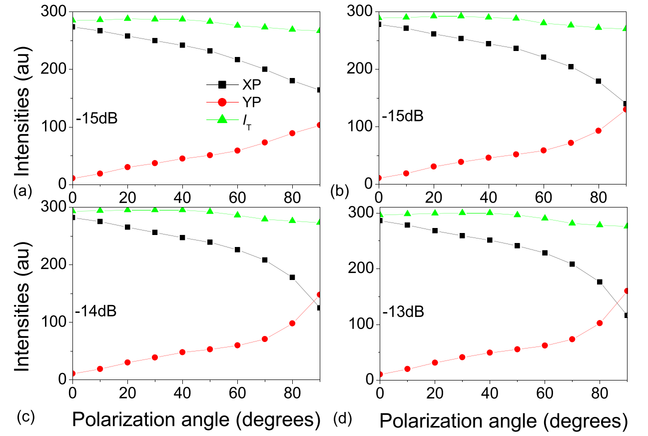

Fig. 5. Polarization-resolved intensities versus θ_p for the configuration A for fixed OF levels at: (a) −15.6, (b) −15, (c) −14, and (d) −13 dB.

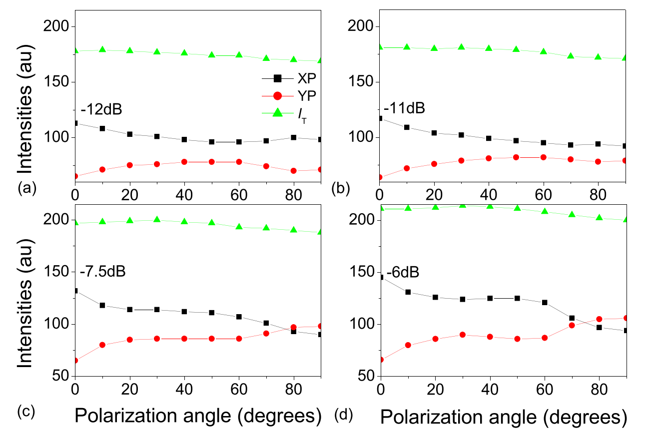

Fig. 6. Polarization-resolved intensities versus polarization angle for the configuration B, for OF fixed at: (a) −12, (b) −11, (c) −7.5, and (d) −6 dB.

1) Case A: For the configuration A, the polarization-resolved intensities as a function of θ_p are shown in Fig. 5 for a range of OF levels of −15.6, −15, −14 and −13 dB. Fig. 5 shows that the XP (YP) mode decreases (increases) gradually with increasing θ_p. Moreover, higher levels of OF lead to PS between VCSEL's modes, as shown in Figs. 5(c) and (d). The PS position is dependent on the OF level and θ_p, where a smaller θ_p is required to implement PS when the OF level increases.

As a result, the total emission intensity began to decreases when θ_p increase. The results illustrate that a smaller polarization angle is required to realize PS when the OF level increases. The experimental results are in good agreement with the previous theoretical analysis [22], which predicted that for a relatively larger feedback level the OF and the gain compete for the dominant effect.

2) Case B: For the configuration B, the polarization resolved output intensities as a function of θ_p dependant on the OF level are displayed in Fig. 6. It can be observed from Fig. 6 that as θ_p increases over a range of $0^0 \leq \theta_p \leq 20°$, the intensity of the XP mode decreases, whilst that of the YP mode increases.

Furthermore, increasing θ_p beyond 20° leads to the decrease in the intensity of the XP mode and the total intensity.

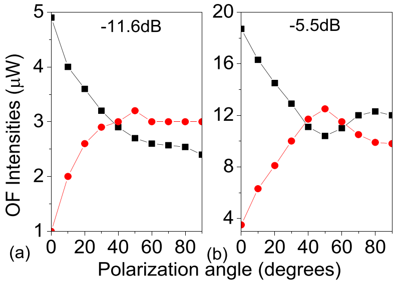

Fig. 7. Feedback strength versus the polarization angle for the configuration B (XP- & YP- optical feedback) at a) −11dB and b) −5.5dB.

However, when the feedback level increases the polarization properties are different than the case with lower feedback levels. For the feedback levels of −7.5 dB and -6 dB, PS occurs and its location is based on the OF level. At a feedback level of −7.5 dB PS is located at θ_p of about 76°, see Fig. 6(c), which moves down to 74° at an OF level of -6 dB as in Fig. 6(d). This illustrates that VCSEL with a higher feedback level requires a smaller θ_p to achieve PS.

Further explanation for above results in Fig. 6 can be obtained via consideration of the feedback effects on the XP and YP modes as in Fig. 7. The feedback intensities of the XP and YP modes have sinusoidal dependency on θ_p. Increasing θ_p leads to decrease (increase) in the feedback intensity of the XP (YP) mode, see Fig. 7(b). This is because of the fact that the feedback strength of the XP and the YP modes become comparable and at relatively smaller OF levels (i.e., −12 and −11 dB) plays less important role than the gain of the XP mode [22]. The θ_p can further affect the feedback lights received by both XP and YP modes in VCSEL.

IV. Theoretical Analysis

The theoretical measurements were obtained using the rate equations deduced from a spin-flip model [14], [17], [19], [20]. In (1-4), only the XP mode was selected to implement the OF for the configuration A. The equations take the form of:

$$\frac{dE_x}{dt} = k(1+i\alpha)[(N-1)E_x + inE_y] - (\gamma_a + i\gamma_p)E_x + \gamma E_x(t-\tau_1)\cos(\theta_p)e^{-i\omega\tau_1} + \sqrt{\beta_{sp}}\xi_x, \quad (1)$$

$$\frac{dE_y}{dt} = k(1+i\alpha)[(N-1)E_y - inE_x] + (\gamma_a + i\gamma_p)E_y + \gamma E_x(t-\tau_1)\sin(\theta_p)e^{-i\omega\tau_1} + \sqrt{\beta_{sp}}\xi_y, \quad (2)$$

$$\frac{dN}{dt} = \gamma_N[\mu - N(1+|E_x|^2+|E_y|^2)+in(E_yE_x^* - E_xE_y^*)], \quad (3)$$

$$\frac{dn}{dt} = -\gamma_s n - \gamma_N[n(|E_x|^2+|E_y|^2) + iN(E_yE_x^* - E_xE_y^*)], \quad (4)$$

where E_x and E_y are the varying amplitudes of the XP and YP modes, respectively. N is the total carrier inversion between conduction and valence bands, whilst n accounts for the difference between carrier inversions with opposite spins. k is the field decay rate, γ_N is the decay rate of N, γ_s is the spin-flip rate, α is the linewidth enhancement factor, μ is the normalized injection current, γ_p is the linear birefringence and γ_a is the linear dichroism, γ is the feedback strengths of XP and YP modes. β_{sp} is the strength of the spontaneous emission, ξ_x and ξ_y are independent Gaussian white noise sources with zero mean and unit variance.

For the configuration B, the equations take the form as in (5-8). For the OF in this model, as in the experiment, both the XP and YP modes were re-injected into the VCSEL. Due to the rotation of QWP, the feedback strength for XP (γ_x) and YP (γ_y) components can be expressed as:

$$\gamma_x = \gamma \times \sqrt{[1+\cos^2(\theta_p)]/2}, \quad \gamma_y = \gamma \times \sqrt{\sin^2(\theta_p)/2}, \quad (5)$$

The rate equations for configuration B can be expressed as [18]:

$$\begin{aligned}\frac{dE_x}{dt} &= k(1+i\alpha)[(N-1)E_x + inE_y] - (\gamma_a + i\gamma_p)E_x \\ &\quad + \gamma_x E_x(t-\tau_2)\cos(\theta_p)e^{-i\omega\tau_2} \\ &\quad - \gamma_y E_y(t-\tau_2)\sin(\theta_p)e^{-i\omega\tau_2} + \sqrt{\beta_{sp}}\xi_x, \quad (6)\\ \frac{dE_y}{dt} &= k(1+i\alpha)[(N-1)E_y - inE_x] + (\gamma_a + i\gamma_p)E_y \\ &\quad + \gamma_x E_x(t-\tau_2)\sin(\theta_p)e^{-i\omega\tau_2} \\ &\quad + \gamma_y E_y(t-\tau_2)\cos(\theta_p)e^{-i\omega\tau_2} + \sqrt{\beta_{sp}}\xi_y, \quad (7)\end{aligned}$$

The feedback level can be calculated from:

$$\gamma = \frac{1-R_0}{\tau_{in}}\sqrt{\frac{R_m}{R_0}}, \quad (8)$$

where $\tau_{in} = 2Ln_o/c$, n_o is the refractive index, L is the cavity length, R_o is the facet reflectivity, $R_m = 10^{F/10}$ represents the external reflectivity, and F (in dB) is the OF level that used in the experiment. Some parameter values are chosen with as a typical value of $\gamma_a = 0.1\text{ns}^{-1}$, $k = 300\text{ns}^{-1}$, $\gamma_N = 1\text{ns}^{-1}$, $\gamma_s = 50\text{ns}^{-1}$, $\gamma_p = 30\text{ns}^{-1}$, $\alpha = 3$, and $\beta_{sp} = 10^{-5}\text{ns}^{-1}$. The experimental parameter values are $\mu = 1.2$, $\lambda = 850$nm, $\tau_1 = 6.4$ ns, the delay of OF in configuration A $\tau_2 = 2.6$ns, the delay time of the OF in configuration B, $R_o = 0.995$, $L = 2\ \mu$m, and $n_o = 3.5$.

A. Numerical Results of Configuration A

Figure 8 shows the numerical results of the average intensities of the XP and YP modes versus the OF coefficient for the configuration A for a range of θ_p. From the figure, it can be observed that behaviours of the polarization modes are comparable with the corresponding experimental measurements as in Fig. 3. At $\theta_p = 0°$ the XP and XY are the dominant and suppressed modes, respectively. The two polarization modes exhibit similar tendency for other values of θ_p as demonstrated in practical measurements. PS occurs at the OF coefficient of 22 ns^{-1}, which is the same point as in practical measurements, see Fig. 3(d). Furthermore, for the configuration A, Fig. 9 shows the numerical results of the polarization-resolved intensities of the XP and YP modes as a function of θ_p when the VCSEL is subjected to different OF levels. It is shown that, for the OF coefficient of 17 ns^{-1} (~ -16 dB) once again the XP and YP are the dominant mode and suppressed modes, respectively.

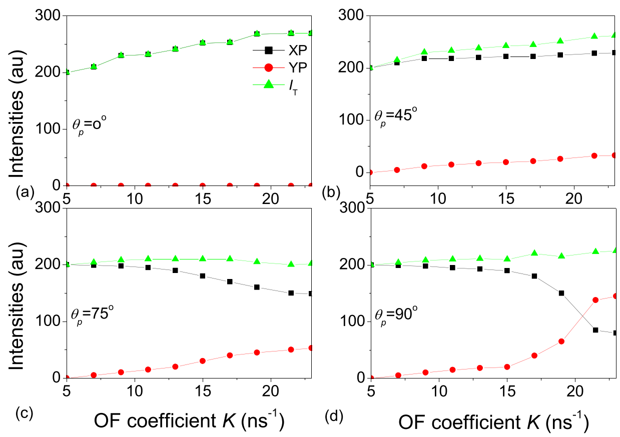

Fig. 8. Numerical results of the polarization-resolved intensities of the XP and YP mode with total output intensity as a function of the OF coefficient for θ_p of: (a) 0°, (b) 45°, (c) 75°, and (d) 90°, for the configuration A model. The squares (circles) line corresponds to the intensity of XP (YP) mode and the green line is the total intensity. The curves for the XP mode and the total output power in (a) are overlapped.

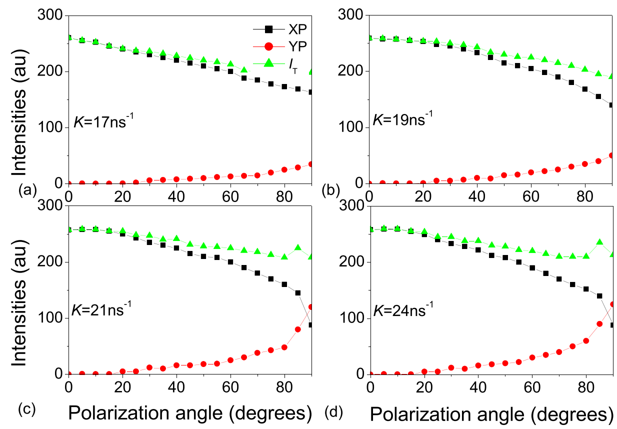

Fig. 9. Numerical results of the polarization-resolved intensities of the XP and YP mode as a function of θ_p at OF coefficients of: (a) 17, (b) 19, (c) 21, and (d) 24 ns^{-1} for the configuration A. The other descriptions are the same as in Fig. 8.

Increasing the feedback level to 24 ns^{-1}(~ -13 dB) results in PS taking place at θ_p of $\sim$87°, which is the same angle that was observed in the experimental measurement, see Fig 5. The results illustrate that for the configuration A there is a good agreement between the predicted and measured results, see Figs. 3 and 5.

B. Numerical Results of Configuration B

Based on the experimental results shown in Fig. 4 for the configuration B, the predicted results for the XP and YP modes intensities versus the OF level are depicted in Fig. 10. For $\theta_p = 0°$ the XP and YP modes exhibit similar behaviours as in Fig. 4(a). In Fig. 10, for different values of θ_p, the XP is still the dominant mode compared with the entire region of OF coefficient and with no PS being observed. The two polarization modes become close to each other at θ_p of 90° for OF of 47 ns^{-1}(~ -7 dB), which is similar to Fig. 4(d).

Fig. 11 presents the numerical measurements of the polarization resolved intensities of the XP and YP modes as a

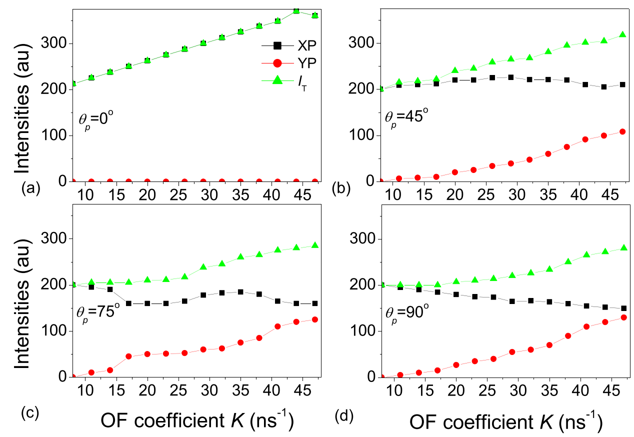

Fig. 10. Numerical results of the polarization-resolved intensities as functions of OF coefficient for θ_p of: (a) 0°, (b) 45°, (c) 75°, and (d) 90° for the configuration B.

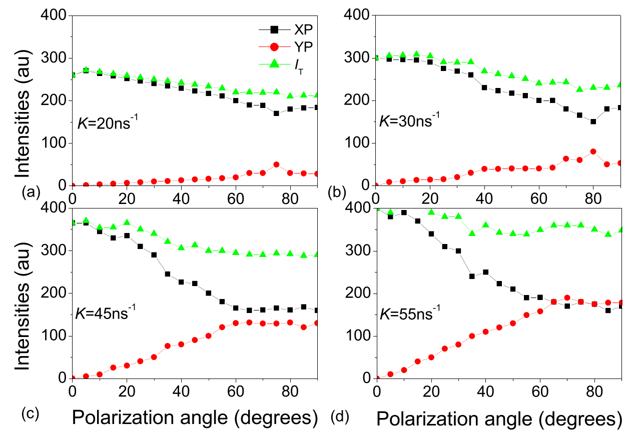

Fig. 11. Numerical results of the polarization-resolved intensities as functions of θ_p corresponding to different feedback levels of: (a) 20, (b) 30, (c) 45, and (d) 55 ns^{-1} for the configuration B.

function of θ_p for OF levels of 20, 30, 45, and 55 ns^{-1} for the configuration B. The corresponding experimental results are illustrated in Fig. 6. Similar tendency of the XP and YP modes in the numeral results can be observed compared to the experimental finding as in Fig. 6. However, PS is observed at slightly different θ_p of $\sim$ 68°for an OFlevel of 55 ns^{-1}(-6 dB), which is lower than f the experimental result ($\sim$74°).

This is because, for higher levels of OF multiple feedbacks may needed as part of the theoretical model.

V. Conclusion

In this study, the effects of the rotated polarization angle θ_p of the OF on the polarization properties of a VCSEL were investigated theoretically and experimentally. Two different configurations of OF were considered. For the configuration A, the parallel mode (XP mode) was re-injected back into the VCSEL whereas in the configuration B two polarization modes (i.e., XP and YP) were re-injected back into the VCSEL. The results showed that in the configuration A there is a good agreement between measured and predicted results, whereas this was not the case with the configuration B, where it was observed 6° some difference between experimental and theoretical results for the PS position. This difference can be attributed to multiple OF due to the optical equipment of the setup, which have caused an experimental error. Furthermore, when no PS was observed, the modes intensities were found to be the same at higher OF levels.

The theoretical and experimental measurements of the polarization properties under rotating polarization angle demonstrated that VCSEL with a high OF level will require a smaller θ_p to achieve PS. For rotating θ_p of the OF VCSEL exhibited PS at a fixed I_B and the OF level. Moreover, the experimental measurements demonstrated the theoretical predictions that the larger θ_p leads to the PS takes place. Additionally, for higher values of θ_p the suppressed mode (YP) is being emitted as in the configuration A. For relatively low levels of OF the polarization modes properties were less affected when changing θ_p. On the other hand, for the configuration A, the PS was observed when the difference between the feedback strengths of the two modes was high enough.

ACKNOWLEDGMENT

The authors would like to thank S. Xiang for her support in the theoretical part.

REFERENCES

[1] S. Ura, S. Shoda, K. Nishio, and Y. Awatsuji, "In-line rotation sensor based on VCSEL behavior under polarization-rotating optical feedback," *Opt. Exp.*, vol. 19, no. 24, pp. 23683–23688, 2011.

[2] K. M. Cuomo and A. V. Oppenheim, "Circuit implementation of synchronized chaos with applications to communications," *Phys. Rev. Lett.*, vol. 71, p. 65, Jul. 1993.

[3] S. Nazhan, Z. Ghassemlooy, and K. Busawon, "Chaos synchronization in vertical-cavity surface-emitting laser based on rotated polarization-preserved optical feedback," *Chaos, Interdiscipl. J. Nonlinear Sci.*, vol. 26, no. 1, p. 013109, 2016.

[4] R. Michalzik, *VCSELs: Fundamentals, Technology and Applications of Vertical-Cavity Surface-Emitting Lasers*. Berlin, Germany: Springer, 2013.

[5] D. V. Kuksenkov and H. Temkin, "Polarization related properties of vertical-cavity surface-emitting lasers," *IEEE J. Sel. Topics Quantum Electron.*, vol. 3, no. 2, pp. 390–395, Apr. 1997.

[6] J. Martin-Regalado, F. Prati, M. S. Miguel, and N. Abraham, "Polarization properties of vertical-cavity surface-emitting lasers," *IEEE J. Quantum Electron.*, vol. 33, no. 5, pp. 765–783, May 1997.

[7] A. Chavez-Pirson, H. Ando, H. Saito, and H. Kanbe, "Polarization properties of a vertical cavity surface emitting laser using a fractional layer superlattice gain medium," *Appl. Phys. Lett.*, vol. 62, no. 24, pp. 3082–3084, 1993.

[8] K. D. Choquette, R. P. Schneider, K. L. Lear, and R. E. Leibenguth, "Gain-dependent polarization properties of vertical-cavity lasers," *IEEE J. Sel. Topics Quantum Electron.*, vol. 1, no. 2, pp. 661–666, Jun. 1995.

[9] S. Nazhan, Z. Ghassemlooy, K. Busawon, and A. Gholami, "Suppressing the nonlinearity of free running VCSEL using selective-optical feedback," *IEEE Photon. Technol. Lett.*, vol. 28, no. 2, pp. 185–188, Jan. 15, 2016.

[10] P. S. Spencer, C. R. Mirasso, and K. A. Shore, "Effect of strong optical feedback on vertical-cavity surface-emitting lasers," *IEEE Photon. Technol. Lett.*, vol. 10, no. 2, pp. 191–193, Feb. 1998.

[11] C. Masoller and N. B. Abraham, "Polarization dynamics in vertical-cavity surface-emitting lasers with optical feedback through a quarter-wave plate," *Appl. Phys. Lett.*, vol. 74, no. 8, pp. 1078–1080, Feb. 1999.

[12] X. F. Li, W. Pan, B. Luo, D. Ma, and G. Deng, "Static and dynamic characteristics of VCSELs with polarisation-selective optical feedback," *IEE Proc.-Optoelectron.*, vol. 153, no. 2, pp. 67–74, Apr. 2006.

[13] Y. C. Chung and Y. H. Lee, "Spectral characteristics of vertical-cavity surface-emitting lasers with external optical feedback," *IEEE Photon. Technol. Lett.*, vol. 3, no. 7, pp. 597–599, Jul. 1991.

[14] J. Paul, C. Masoller, Y. Hong, P. S. Spencer, and K. A. Shore, "Impact of orthogonal optical feedback on the polarization switching of vertical-cavity surface-emitting lasers," *J. Opt. Soc. Amer. B, Opt. Phys.*, vol. 24, no. 8, pp. 1987–1994, 2007.

[15] K. D. Choquette, K. Lear, R. Leibenguth, and M. Asom, "Polarization modulation of cruciform vertical-cavity laser diodes," *Appl. Phys. Lett.*, vol. 64, no. 21, pp. 2767–2769, 1994.

[16] Y. Hong, P. S. Spencer, and K. A. Shore, "Suppression of polarization switching in vertical-cavity surface-emitting lasers by use of optical feedback," *Opt. Lett.*, vol. 29, no. 18, pp. 2151–2153, 2004.

[17] M. A. Arteaga *et al.*, "Study of polarization properties of VCSELs subject to optical feedback from an extremely short external cavity," in *Proc. CLEO/Europe Conf. Lasers Electro-Opt. Eur.*, Jun. 2005, p. 148.

[18] N. Shibasaki, A. Uchida, S. Yoshimori, and P. Davis, "Characteristics of chaos synchronization in semiconductor lasers subject to polarization-rotated optical feedback," *IEEE J. Quantum Electron.*, vol. 42, no. 3, pp. 342–350, Mar. 2006.

[19] S. Xiang *et al.*, "Variable-polarization optical feedback induced hysteresis of the polarization switching in vertical-cavity surface-emitting lasers," *J. Opt. Soc. Amer. B, Opt. Phys.*, vol. 27, no. 12, pp. 2512–2517, 2010.

[20] S. Y. Xiang *et al.*, "Quantifying chaotic unpredictability of vertical-cavity surface-emitting lasers with polarized optical feedback via permutation entropy," *IEEE J. Sel. Topics Quantum Electron.*, vol. 17, no. 5, pp. 1212–1219, Sep./Oct. 2011.

[21] L. Khaykovich, T. Galfsky, Z. Shotan, and N. Gross, "TE-TM coupled mode dynamics in a semiconductor laser subject to feedback with variably rotated polarization," *Opt. Commun.*, vol. 282, no. 10, pp. 2059–2061, 2009.

[22] S. Xiang, W. Pan, L. Yan, B. Luo, N. Jiang, and L. Yang, "Polarization properties of vertical-cavity surface-emitting lasers subject to feedback with variably rotated polarization angle," *Appl. Opt.*, vol. 48, no. 27, pp. 5176–5183, 2009.

[23] J. Martín-Regalado, S. Balle, and M. S. Miguel, "Polarization and transverse-mode dynamics of gain-guided vertical-cavity surface-emitting lasers," *Opt. Lett.*, vol. 22, no. 7, pp. 460–462, 1997.

[24] S. Nazhan, Z. Ghassemlooy, K. Busawon, and A. Gholami, "Investigation of polarization switching of VCSEL subject to intensity modulated and optical feedback," *Opt. Laser Technol.*, vol. 75, pp. 240–245, Dec. 2015.

[25] S. Nazhan, Z. Ghassemlooy, and K. Busawon, "Harmonic distortion dependent on optical feedback, temperature and injection current in a vertical cavity surface emitting laser," *J. Phys. D, Appl. Phys.*, vol. 49, no. 14, p. 145107, 2016.

[26] R. Yi *et al.*, "Long-wavelength VCSEL using high-contrast grating," *IEEE J. Sel. Topics Quantum Electron.*, vol. 19, no. 4, p. 1701311, Jul./Aug. 2013.

Salam Nazhan (M'13) was born in Baqubah, Iraq in 1971. He received the B.S. and M.S. degrees in physics, and electronics physics from Al Mustansiriya University, Baghdad, Iraq, in 1998 and 2005, respectively, and the Ph.D. degree in optoelectronics from Northumbria University, Newcastle upon Tyne, U.K., in 2016. He joined the Optoelectronics Research Group as a Researcher at Bangor University, Wales, U.K., from 2011 to 2012, and the Optical Communications Research Group at Faculty of Engineering and Environment, Northumbria University, until 2016. He is currently a Lecturer and the Principal Investigator of a number of undergraduate students with the Power and Electrical Engineering Department, University of Diyala, Iraq. He already published around 14 papers. His research focuses on optical and electrical characteristic of vertical-cavity surface emitting laser for free space optical communications. His current research interests include characterizations, optical chaotic signal, and nonlinearity behaviors of VCSEL. He became a member of the Iraqi Physicists Society in 2005, and the Iraqi Higher Education Society in 2004. He is a Technical Committee Member and presented his research in several international conferences.

Zabih Ghassemlooy (SM'92) received the B.Sc. degree (Hons.) in electrical and electronics engineering from Manchester Metropolitan University, Manchester, U.K., in 1981, and the M.Sc. and Ph.D. degrees from the Institute of Science and Technology, University of Manchester, Manchester, U.K., in 1984 and 1987, respectively. From 1987 to 1988, he was a Post-Doctoral Research Fellow with City University, U.K. In 1988, he joined Sheffield Hallam University as a Lecturer, becoming a Reader in 1995 and a Professor in optical communications in 1997. In 2004, he joined the University of Northumbria (UNN), Newcastle upon Tyne, U.K., as an Associate Dean (AD) for research with the School of Computing, Engineering, and Information Sciences, and from 2012 to 2014, he was an AD of Research and Innovation, Faculty of Engineering, UNN, where he is currently the Head of the Northumbria Communications Research Laboratories within the faculty. In 2016, he became a Research Fellow at the Chines Academy of Science, and since 2015, has been a Distinguished Professor with the Chinese Academy of Sciences, Quanzhou, China. He was a Visiting Professor with University Tun Hussein Onn Malaysia, Malaysia, from 2013 to 2017. He is currently a Visiting Professor with Huaqiao University, Quanzhou, China. He has authored over 675 papers (over 251 journals and 6 books), over 85 keynote and invited talks, and has supervised 55 Ph.D. students. His current research interests include optical wireless communications, free space optics, and visible light communications. He is a member of the OSA. He is the fellow of the IET. In 2001, he was a recipient of the Tan Chin Tuan Fellowship in engineering from Nanyang Technological University, Singapore. He was the Vice-Chair of the EU Cost Action IC1101 from 2011 to 2016. He has been the Chair of colloquium on Optical Wireless Communications (OWC) as part of the IEE/IET CSNDSP Symposium since 2008. He was the Organizer/Co-Organizer of the Workshop on the OWC IEEE ICC from 2015 to 2017. He has been the Chair of colloquium on OWC as part of the IEE/IET CSNDSP Symposium since 2008, and a number of international colloquiums/workshops. From 2004 to 2006, he was the IEEE UK/IR Communications Chapter Secretary, the Vice-Chairman from 2004 to 2008, the Chairman from 2008 to 2011, and the Chairman of the IET Northumbria Network from 2011 to 2015. He is the Chief Editor of the *British Journal of Applied Science and Technology* and the *International Journal of Optics and Applications*. He has been the Quest Editor of a number of special issues in the IEEE and IET journals. He is a Co-Author of a CRC Book on *Optical Wireless Communications—Systems and Channel Modeling with MATLAB* (2012), and the Co-Editor of three books, including the Springer book on *Optical Wireless Communications—An Emerging Technology* (2016), and the IET book on *Analogue Optical Fibre Communications* and the *IEE Telecommunication series 32* (1995). He is the Founder and the Chairman of the IEEE, the IET International Symposium on Communication Systems, Network and Digital Signal Processing.